Volume 1 | Number 1 | Jan 2013 | Pages 1–100

Journal of
Materials Chemistry A

Materials for energy and sustainability
www.rsc.org/materialsA

Li⁺

ROYAL SOCIETY OF CHEMISTRY

ROYAL SOCIETY OF CHEMISTRY

www.rsc.org/materialsA

Journal of Materials Chemistry A

RSCPublishing

ARTICLE

CuO Nanoleaves Enhance c-Si Solar Cell Efficiency

Yusheng Xia, Xuxin Pu, Jie Liu, Jie Liang, Pujun Liu, Xiaoqing Li and Xibin Yu*

Variety-sized arrays of CuO nanoleaves (NLs) were fabricated on the pyramid-textured c-Si wafer. The CuO NLs/c-Si solar cells show a great increase of the optical absorption and a reduction of the reflectance in the 250-1250 nm wavelength range, compare to the reference one. The c-Si solar cell integrated with CuO NLs generates the graded index of refraction between the surface of Si and air, and improves light utilization efficiency by increasing the light-trapping effect and forming the resonant optical modes, which makes the multiple scattering of the incident light. In addition, the deposition of p-type CuO NLs on the surface of Si wafer can form CuO NLs/c-Si junction and generate a built-in potential, which is beneficial for the separation of photogenerated electrons and holes, leading to the minority carrier lifetime (τ_{eff}) increase from 5.7 to 15.0 μs. The CuO NLs/c-Si structure both reduces optical loss and improves carrier collection, distinctly enhance c-Si solar cell efficiency. The experimental results indicate that short-circuit current, and power conversion efficiency of CuO NLs/c-Si solar cell increase by 10.30% and 17.90%, respectively. CuO NLs/c-Si structure is expected to exceed the Shockley-Queisser limit of the single junction solar cell.

1. Introduction

It is well known that 90 % of commercial PV modules manufactured worldwide are made of solar-grade Si owing to its high natural abundance, mature processing technology, and excellent reliability in solar cells.[1-3] Commercial Si PV has been developed to convert sunlight into electricity at efficiencies around 18%. However, it is challenging for us to develop Si solar cells with higher efficiency. Main limiting factors for the conversion efficiency of Si solar cells are optical loss, recombination, and thermal or quantum losses.[4-7] A large portion of the energy loss during solar-cell operation is attributed to optical loss.[8, 9] The polished substrates reflect approximately 30-35% of incident sunlight for wavelengths corresponding to energies larger than the band gap of silicon due to the low absorption coefficient of silicon.[10] Therefore, the optical loss of solar cells greatly affects their performances. Thus, an antireflection coating is especially important in Si solar cells.[11-13] Besides, the carrier recombination is also a key limiting factor for the performance of Si solar cells. The easy recombination of photogenerated carriers with surface defects can lead to inferior cell efficiency.[14-18] The array nanostructures, such as ZnO NWs,[19-22] Silicon nanowires,[2, 23] InP Nanowire,[24] In$_2$O$_3$ Nanopushpins,[25] and indium tin oxide nanowhisker,[26] not only improved light absorption via light trapping effect,[27, 28] but also facilitated the collection of the photocarrier[29], which opened up a new area in developing advanced functional materials and photo-voltage device,[30, 31] etc. CuO is an environment-friendly oxide semiconductor material with a wide energy gap of ~1.4 eV.[32] As a p-type semiconductor,[33] CuO Nanoleaves with the excellent optical absorption capacity can generate the graded index of refraction between the surface of Si and air and form CuO NLs (p-type)/Si (n-type) junction in c-Si interface. So far, optical properties of CuO nanostructures directly growing on the surface of c-Si solar cell have rarely been studied. In this study, we fabricated a variety-sized array of CuO NLs on the pyramid-

textured c-Si solar cell. It is found that the characteristic of CuO nanoleaves offers a broad-band light harvesting from visible to near infrared (IR). Furthermore, we demonstrate that the CuO NLs (p-type)/c-Si (n-type) junction can suppress the recombination of the photogenerated carriers, improve the open circuit voltage of Si solar cells. Therefore, the CuO NLs /c-Si solar cells can significantly increases the short-circuit current (J_{sc}) and enhances the power conversion efficiency. The cost effective and environmentally friendly technology can be easily applied to the industrial scale production of Si solar cells. The CuO NLs/c-Si solar cells expected to exceed the Shockley-Queisser limit of the single junction solar cells.

2. Results and discussion

Figure 1 (a–d) show the surface morphologies of CuO NLs with different lengths, widths, and densities of NLs growing on
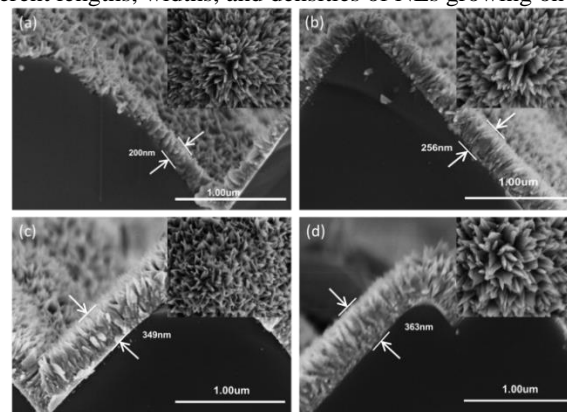
Figure 1. Cross-sectional view of FESEM morphologies of the CuO NLs growing on pyramid-textured Si substrates for (a) 30 min; (b) 45 min; (c) 60 min and (d) 90 min, respectively. Insert: top view.

Journal of Materials Chemistry A Accepted Manuscript

pyramid-textured Si substrates.

The compact and uniform CuO NLs are vertically aligned on the pyramid-textured Si substrates. The CuO NLs become relatively longer upon the increase of the growth time. SEM indicates that the length of the NLs is between ~200 and ~363 nm, and their width is between 69 nm and 97 nm. The morphology of CuO NLs can be controlled by adjusting the thickness of seed-layer and the corresponding growth parameters.
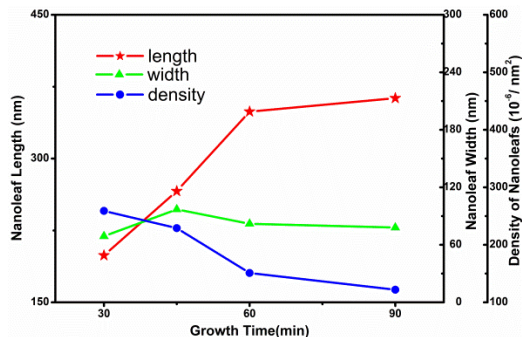
Figure 2. Plots of average length, width, and density of CuO NLs as a function with the growth time.

As shown in Figure 2, CuO NLs have an average width of ~69 nm, length of ~200 nm, and density of ~259×10^{-6} NLs /nm^2 as the growth time is 30 min. With extending growth time, the length of NLs increase steadily, the width of CuO NLs remain almost unchanged, and the NLs density show a small decrease due to the increase of lengths and the dissolution of small NLs. As growth time is prolonged to 60 min, the length of CuO NLs increased to ~363 nm, and the density declined to ~122×10^{-6} NLs /nm^2.
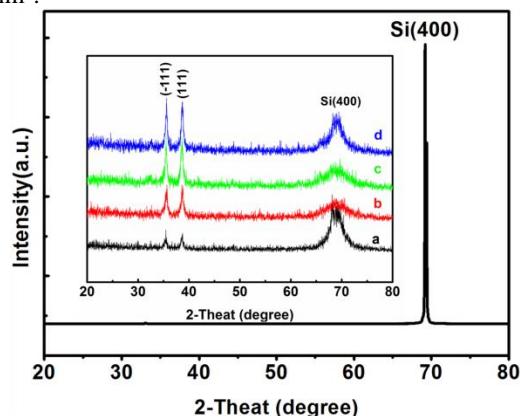
Figure 3. XRD patterns of CuO NLs growing on c-Si wafers. The growth time: (a) 30 min; (b) 45 min; (c) 60 min; (d) 90min.

The XRD patterns in Figure 3 indicate that the as-prepared product is monoclinic CuO nanocrystalline. Two strong diffraction peaks at 35.50 ° and 38.73 °can be indexed to {-111}, {111} of monoclinic CuO crystal (JCPDS card no. 49-0937) and indicate that CuO NLs have a well crystallinity. It can also be found that the longer reaction time caused the stronger diffraction peak for CuO NLs. The pyramid-textured Si has a strong diffraction peaks at 69.13 °, corresponding to the monocrystalline Si structure. With the growth of CuO NLs, this Si peak became gradually wider. Also, no characteristic peaks of impurities were detected in the pattern.

The growth of CuO NLs involves an evolution of the structural complexity from 0-D nanoparticles to 1-D nanorod, and then to 2-D 'nanoleaf' structures. The original attachment goes through all of these processes with the help of the CuO seeds. The two peaks at 35.50 ° and 38.73 ° become stronger as the time increase. This result indicates that Cu^{2+} and O^{2-} ions grow crosswise and fuse into each other with crystallographic orientation of (111) and (-111) planes to form 1-D nanorods first, and then tend to align sequentially with each other perpendicular to the [111] direction. Then, the 1-D nanorods are parallel to each other to form 2-D CuO NLs.
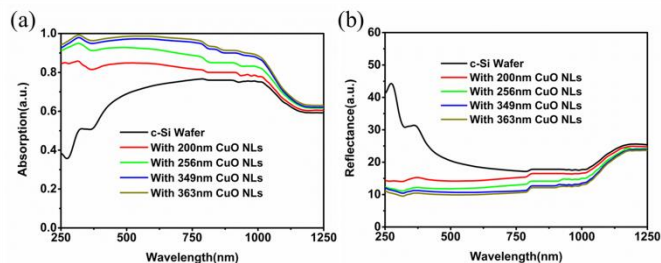
Figure 4. (a) UV-vis-IR absorption and (b) reflectance spectra of CuO nanoleaves with different growth time on pyramid-textured Si substrates.

Generally speaking, the c-Si wafer cannot sufficiently absorb all sunlight photons for wavelengths corresponding to energies larger than the band gap of silicon. In this study, we found that optical absorption (as shown in Figure 4a) of the c-Si solar cell with CuO NLs greatly increase in the wavelength range between 250 and 1250 nm, compare to the reference one. Obviously, the enhancement of optical absorption will result in the improvement of light utilization efficiency. In addition, this array structure can cause optical resonance and the multiple scatterings of the incident light between the CuO NLs, which can effectively absorb, trap incident light at their optically resonant wavelength. So, most light in the investigated wavelength range can be captured by the c-Si wafer integrated with CuO NLs due to the broad band absorption and light scattering of the CuO NLs. With prolonging the length of nanoleaves, the absorption gradually increase and the reflectance gradually decrease due to the light-scattering enhancement effect of CuO nanostructures. Besides, the surface area of the wafer becomes larger with increasing the length of NLs, which are beneficial to the absorption. When growth time increased from 60 to 90 min, the length of CuO NLs only increases a little. It means that the absorption and light-trapping almost reach the limit. If the CuO NLs are too long, an excessive surface defect promotes recombination of photogenerated electrons and holes into CuO NLs and suppresses the power conversion efficiency of the CuO NLs/c-Si solar cell. With CuO NLs growing for 90 min, reflectivity of the CuO NLs/c-Si solar cells decrease from 17.18 to 9.7%, compare to the bare Si wafer, which show a relative improvement of almost 43% (as shown in Figure 4b). The CuO NLs growing on the pyramid-textured c-Si provide broad band reflection suppression with very little wavelength dependence, which allow a gradually and continuously change of the effective refractive index from Si to air, and improve the optical impedance matching at the interfaces. Consequently, the CuO NLs as a graded index layer within the hierarchical structure can effectively eliminate the Fresnel reflection over the broad spectral width. The reflectivity of CuO NLs/c-Si solar cells decreases with the length increase of NLs array.
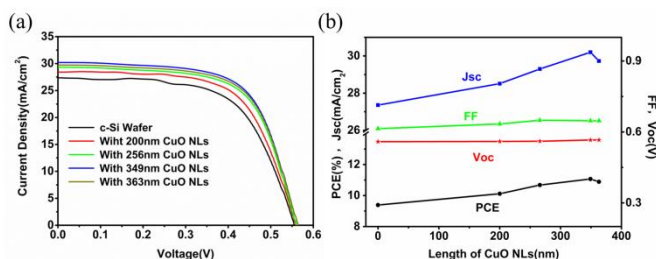
Figure 5. (a) J−V characteristics of variety-sized CuO NLs /c-Si solar cells. (b) Comparison of PEC, J_{sc}, FF, and V_{oc} for CuO NLs/c-Si solar cells.

The performances of CuO NLs/c-Si solar cells were characterized by the J–V curves under the condition of AM 1.5 illumination (as shown in Figure 5a). The main photovoltaic parameters are summarized in Table 1. All the photovoltaic parameters of the optimized CuO NLs/c-Si solar cells have a distinct enhancement, compare to the one without CuO NLs.

The characteristics of short-circuit current density (J_{sc}) demonstrate the enhancement of the CuO NLs/c-Si solar cells from 27.36 to 30.20 mA/cm^2, compare to the reference one. The short-circuit current density is proportional to the conversion efficiency from incident photons to electrical current. The increase of short-circuit current density are ascribed to the absorption enhancement and the reflectance decline. When the CuO NLs were deposited on pyramid-textured Si substrates, the composite structure is beneficial to light-trapping and reduces reflectivity, which can increase the concentrations of effective photon and then enhance the photocurrent of the cells. However, when the growth time increase from 60 to 90 min, J_{sc} turn to decline slightly. It indicates that not all of the absorbed photons can be effectively converted to electric energy.

Table 1. Photovoltaic parameters of CuO NLs/c-Si Solar Cells.

Sample	J_{sc}[mA/cm^2]	V_{oc}[V]	FF[%]	η[%]	Δη(%)
Si	27.36	0.559	61.41	9.39	-----
30min	28.51	0.560	63.39	10.12	7.8
45min	29.30	0.561	64.97	10.68	13.7
60min	30.20	0.566	64.76	11.07	17.9
90min	29.73	0.566	64.72	10.89	16.0

Open circuit voltage (V_{oc}) exhibits an increase from 0.559 to 0.566 mV for c-Si solar cells integrated with CuO NLs, and the power conversion efficiency of the photovoltaic device enhances from 9.39 to 11.07%, compare to the reference one. Figure 5b shows that PCE and J_{sc} are consistently changeable with the length of CuO NLs, while the open-circuit voltage (V_{oc}) and FF are essentially independent of length of CuO NLs.
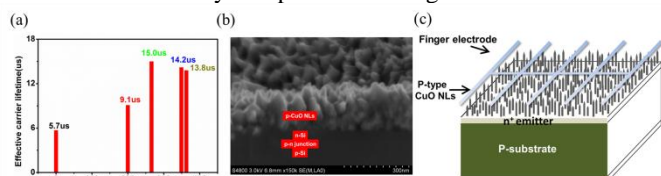
Figure 6. (a) Comparison minority-carrier lifetime of the different lengths of CuO NLs/c-Si solar cells. (b) The p-n-p junction of CuO NLs/c-Si solar cells. (c) Schematic of the pyramid-textured Si Solar Cells Integrated with CuO NLs.

The experimental results show that the CuO NLs/c-Si junction solar cells can suppress the recombination of charge carriers, improving carrier collection, and then increasing photoelectric conversion efficiency. The p-type CuO NLs and n-type Si interface forms a p-n junction, which is beneficial for the spatial separation of photogenerated electrons and holes under the action of the built-in potential formed by the CuO NLs /c-Si junction. Figure 6b shows the p-n-p junction model, the CuO NLs thin film acts as a light-transmitting p-type emitter, and photocarriers are separated under the action of the built-in potential form by the CuO/c-Si structure and are easily transmit into Si junction from the conduction band of CuO NLs. Each NL in the array direction can form p-n-p junction with the c-Si substrate, acting as a tiny solar cell, in which the photogenerated carriers transport fast along the long axis, and only have to travel across a short pathway to reach the charge-separating junction. Figure 6a shows the comparison of minority-carrier lifetime of the different lengths of CuO NLs with different lengths. Upon growth of CuO NLs on the surface of c-Si wafer, surface recombination is very effectively suppressed, and τ_{eff} substantially increased from 5.7 to 15.0 μs. However, when continue to increase the length of the CuO NLs, the surface area increase, which induce more defect or minority carrier recombination centers at the c-Si surface. Besides, diffusion path length of minority carrier transfers in the NLs along the vertical direction also increases. As a result, recombination in the transfer process increases to cause poor interface charge carrier collection efficiency, which offsets the improvement of light-trap effect. CuO NLs/c-Si structure can not only improve optical utilization, but also facilitate photocarrier collection. Therefore, we should consider the conflicting factors to reduce surface recombination and improve the light-trapping effectiveness for longer CuO NLs. In order to achieve the optimal power conversion efficiency, the CuO NLs lengths were adjusted to find an optimal length. Appropriately long CuO NLs can make the Si solar cells perform well.

3. Experimental

Slices (3.0×3.0 cm^2) of c-Si wafers without Si$_3$N$_4$, which purchased from Changzhou Yijing Optoelectronics Technology Co., Ltd, were applied in this work. The thickness of wafers is 200 μm with bulk p-n junction. The resistivity of Si wafer is in the range of 1-10 Ω·cm. The surfaces of wafers were first cleaned to eliminate any metal impurities and anything organic. All the chemical reagents were purchased from Aladdin and used without further purification. The aqueous solutions were prepared using double distilled water. 10 mM copper acetate monohydrate [Cu(CH$_3$COO)$_2$·H$_2$O, AR] in ethanol was prepared as the A solution (the seed solution). 0.02M copper nitrate trihydrate [Cu(NO$_3$)$_2$·3H$_2$O, AR] and 0.02M hexamethylenetetramine (HTMA, AR) in water was prepared as the B solution (the growth solution).

The surface morphology and size distribution of vertically aligned CuO nanoleaves were characterized by field-emission scanning electron microscopy [FESEM, S-4800 Hitachi]. The absorption and reflection spectra of the CuO NLs/c-Si wafers samples were measured using a Varian Carry 500 UV/vis/NIR spectrophotometer with an integrating sphere (Labsphere) in a wavelength range of 250−1250 nm, which corresponds to the

major spectral irradiance of sunlight. The minority carrier lifetime of the samples was measured using a Si wafer life-time WT-2000 PVN. A Keithley (Cleveland, OH) 2440 5A source meter was used to obtain current–voltage characteristics of fabricated solar cells with and without CuO nanoleaves coating. Chemical vapor deposition (CVD) was employed to evaporation Al on the reverse side of the c-Si substrates, Ag grids were then screen-printed on front side, followed by rapid thermal annealing. The total cell area measured is 9 cm^2. A solar simulator [ABET TECHNOLOGIES, AM 1.5G, 1000 W/m^2] was used for illumination during the measurements. The light intensity was calibrated with a silicon standard cell (PV Measurements, Inc.).

CuO nanoleaves on pyramid-textured c-Si substrates were synthesized by two-step method. CuO nanoseed particles were firstly deposited on the surface of Si substrate via an alcohothermal method. The A solution was spin-coated onto the surface of single-crystalline Si substrate at 1600 rpm, and then was heated at 120 $^\circ$C for a minute to dry. The above steps were repeated for several times to obtain a high-density growth of CuO nanoparticles. Then, the Si substrate was transferred into a regular laboratory oven for annealing process at 250 $^\circ$C in air for 30 min to obtain the uniform CuO nanoseeds layer, 10 nm thick CuO films as the seed layers were obtained. The second step is to grow CuO NLs from the seeded Si substrates. The pre-seeded substrates were dipped into the B solution in a vertical position and then heated to 90 $^\circ$C for 30-90 min, HMTA can produce ammonia, and further hydrolyzes to provide OH$^-$, which react with copper nitrate to produce the insoluble copper hydroxides. Then, insoluble copper oxide was formed. All the synthesis process was performed under atmospheric pressure. The final product on the pyramid-textured Si substrate was washed with deionized H$_2$O several times to remove any of residual salts or amine complexes.

Conclusions

In summary, CuO NLs growing on the pyramid-textured Si have been demonstrated to have promising potential for improving the efficiency of c-Si solar cells. The study shows that the CuO NLs/c-Si solar cells can significantly enhance power conversion efficiency. The enhancement is attributed to the enhanced absorption and trapping of sunlight, and generation of the graded index of refraction between the surface of Si and air. The CuO NLs/c-Si structure can form P-N junction in their interface which is beneficial for the spatial separation of photogenerated electrons and holes, besides, carrier collection efficiency can be improved as well. Those superior photovoltaic properties of CuO NLs/c-Si solar cells can be realized by a simple, low-temperature process, and provided a great potential for low-cost, high-efficiency solar cells, expanded the application of copper oxide on Si solar cells by directly depositing it on the pyramid-textured Si surface and provided a potential new photovoltaic technology. CuO NLs/c-Si structure is expected to exceed the Shockley-Queisser limit of the single junction solar cell.

Acknowledgements

Notes and references

The Education Ministry Key Lab of Resource Chemistry and Shanghai Key Laboratory of Rare Earth Functional Materials, Department of Chemistry, Shanghai Normal University, Shanghai 200234, People's Republic of China. 100 Guilin Rd Shanghai Normal University Shanghai, 100 Guilin Rd Shanghai Normal University Shanghai, 200234, China.

1. D. M. Bagnall and M. Boreland, Energ Policy, 2008, 36, 4390-4396.
2. X. Wang, K. Q. Peng, X. J. Pan, X. Chen, Y. Yang, L. Li, X. M. Meng, W. J. Zhang and S. T. Lee, Angew. Chem. Int. Ed. 2011, 50, 9861-9865.
3. C. Xie, X. Zhang, K. Ruan, Z. Shao, S. S. Dhaliwal, L. Wang, Q. Zhang, X. Zhang and J. Jie, Journal of Materials Chemistry A, 2013, 1, 15348-15354.
4. C.-Y. Huang, D.-Y. Wang, C.-H. Wang, Y.-T. Chen, Y.-T. Wang, Y.-T. Jiang, Y.-J. Yang, C.-C. Chen and Y.-F. Chen, ACS Nano., 2010, 4, 5849-5854.
5. A. Polman and H. A. Atwater, Nat. Mater., 2012, 11, 174-177.
6. W. A. Tisdale, K. J. Williams, B. A. Timp, D. J. Norris, E. S. Aydil and X. Y. Zhu, Science., 2010, 328, 1543-1547.
7. P. R. Pudasaini, F. Ruiz-Zepeda, M. Sharma, D. Elam, A. Ponce and A. A. Ayon, ACS Appl. Mater. Interfaces, 2013, 5, 9620-9627.
8. Y. Liu, A. Das, S. Xu, Z. Lin, C. Xu, Z. L. Wang, A. Rohatgi and C. P. Wong, Adv. Energy Mater., 2012, 2, 47-51.
9. A. G. Aberle, Sol. Energy Mater. Sol. Cells., 2001, 65, 239-248.
10. C.-Y. Huang, D.-Y. Wang, C.-H. Wang, Y.-T. Wang, Y.-T. Jiang, Y.-J. Yang, C.-C. Chen and Y.-F. Chen, J. Phys. D: Appl. Phys., 2011, 44, 085103.
11. D. Wan, H.-L. Chen, T.-C. Tseng, C.-Y. Fang, Y.-S. Lai and F.-Y. Yeh, Adv. Funct. Mater., 2010, 20, 3064-3075.
12. L.-K. Yeh, K.-Y. Lai, G.-J. Lin, P.-H. Fu, H.-C. Chang, C.-A. Lin and J.-H. He, Adv. Energy Mater., 2011, 1, 506-510.
13. H. Nagel, A. G. Aberle and R. Hezel, Progress in Photovolt: Res. Appl., 1999, 7, 245-260.
14. H.-C. Y. a. H. M. B. Jihun Oh*, Nat Nano 2012, 7, 1748-3387.
15. S. Avasthi, S. Lee, Y.-L. Loo and J. C. Sturm, Adv. Mater., 2011, 23, 5762-5766.
16. M. C. Putnam, D. B. Turner-Evans, M. D. Kelzenberg, S. W. Boettcher, N. S. Lewis and H. A. Atwater, Appl. Phys. Lett. 2009, 95, 163116.

Journal of Materials Chemistry A Accepted Manuscript

17. J. A. Giesecke, M. C. Schubert, B. Michl, F. Schindler and W. Warta, Sol. Energy Mater. Sol. Cells., 2011, 95, 1011-1018.

18. C. Xie, X. Zhang, Y. Wu, X. Zhang, X. Zhang, Y. Wang, W. Zhang, P. Gao, Y. Han and J. Jie, J. Mater. Chem. A, 2013, 1, 8567-8574.

19. S.-H. Baek, S.-B. Kim, J.-K. Shin and J. Hyun Kim, Sol. Energy Mater. Sol. Cells., 2012, 96, 251-256.

20. Y.-C. Chao, C.-Y. Chen, C.-A. Lin, Y.-A. Dai and J.-H. He, J. Mater. Chem., 2010, 20, 8134.

21. J. Y. Chen and K. W. Sun, Sol. Energy Mater. Sol. Cells., 2010, 94, 930-934.

22. Y. Tak and K. Yong, *J. Phys. Chem. B.*, 2005, 109, 19263-19269.

23. K. Q. Peng and S. T. Lee, Adv. Mater., 2011, 23, 198-215.

24. J. Wallentin, N. Anttu, D. Asoli, M. Huffman, I. Aberg, M. H. Magnusson, G. Siefer, P. Fuss-Kailuweit, F. Dimroth, B. Witzigmann, H. Q. Xu, L. Samuelson, K. Deppert and M. T. Borgstrom, Science., 2013, 339, 1057-1060.

25. C.-Y. Huang, G.-C. Lin, Y.-J. Wu, T.-Y. Lin, Y.-J. Yang and Y.-F. Chen, J. Phys. Chem. C., 2011, 115, 13083-13087.

26. C.-H. Chang, M.-H. Hsu, P.-C. Tseng, P. Yu, W.-L. Chang, W.-C. Sun and W.-C. Hsu, Opt. Express., 2011, 19, A219-A224.

27. E. Garnett and P. Yang, Nano Lett, 2010, 10, 1082-1087.

28. J. Y. Chen, C. Con, M. H. Nano Lett.Yu, B. Cui and K. W. Sun, Acs Appl Mater Interfaces, 2013, 5, 7552-7558.

29. R. Yu, Q. Lin, S.-F. Leung and Z. Fan, Nano Energy., 2012, 1, 57-72.

30. L. Cao, P. Fan, A. P. Vasudev, J. S. White, Z. Yu, W. Cai, J. A. Schuller, S. Fan and M. L. Brongersma, Nano Lett., 2010, 10, 439-445.

31. L. Cao, P. Fan, A. P. Vasudev, J. S. White, Z. Yu, W. Cai, J. A. Schuller, S. Fan and M. L. Brongersma, Nano Lett., 2010, 10, 439-445.

32. A. A. Umar and M. Oyama, Cryst. Growth Des., 2007, 7, 2404-2409.

33. B. J. Hansen, N. Kouklin, G. Lu, I. K. Lin, J. Chen and X. Zhang, J. Mater. Chem. C, 2010, 114, 2440-2447.